Materials and methods

General reagents and solvents were commercially available and used as received. [Ru(*p*-cymene)Cl_2(pta)] (pta = 1,3,5-triaza-7-phospaadamantane), termed RAPTA-C, was synthesized according to the literature method proposed by Allardyce.[1] ^{1}H-NMR spectra were acquired on a 500 MHz Varian Inova Unity Equipment using $CDCl_3$ as solvent. Thermogravimetric and differential calorimetric analyses were performed, under air atmosphere, on a Shimadzu-TGA-50 H/DSC equipment, at a heating rate of 293 K min^{-1}. UV-vis spectra were collected on a Cary Series UV-vis Spectrophotometer. XRPD data were collected on a Bruker D2-PHASER diffractometer (θ - 2θ) using CuKα radiation (λ = 1.5418 Å) and LYNXEYE detector, from 5 to 35 (2θ) and a step size of 0.02. The compounds were manually grinded in an agate mortar, and then deposited in the hollow of a silicon sample holder. N_2 adsorption isotherms were measured at 77 K on a Micromeritics Tristar 3000 volumetric instrument. Prior to measurement, powdered samples were activated by heating at 403 K for 7 h and outgassing to 10^{-6} mbar. HR-TEM analysis was performed using a STEM PHILIPS CM20 HR electron microscope operating at 200 keV with Energy Dispersive X-ray analysis (EDX). Elemental analyses were carried out on a Fisons-Carlo Erba analyzer model EA 1108. ATR data were collected with a Fourier transform infrared spectrophotometer JASCO 6200, using the attenuated total reflectance accessory. RP-HPLC measurement were carried out on a Thermo Scientific Spectra System P4000 with a Hypersil Gold column C-18 reverse-phase (100 x 4.6 nm from Thermo Scientific) and equipped with a Spectra System UV8000, a photodiode array detector (PDA) and ChromQuest 5.0 software. HPLC grade methanol was purchased from J. T. Baker, while the phosphate buffer (0.1 M) used for the HPLC measurements was prepared in ultra pure water with sodium dihydrogen phosphate dehydrated and the pH was adjusted to 3 by adding some drops of HCl (1 M).

Synthesis of $[Fe^{III}_3O(H_2O)_2F\cdot\{C_6H_3(CO_2)_3\}_2nH_2O]$ (n ~14.5) (MIL-100(Fe))

MIL-100(Fe) was prepared from hydrothermal reaction of benzene-1,3,5-tricarboxilic acid (btc) with metallic iron, HF, concentrate nitric acid and H_2O at 433 K for 8 hours as reported.[2] In a typical synthesis, the composition of the reaction mixture was 55.84 mg (1.0 mmol) of Fe(0), 138.7 mg (0.67 mmol) of btc, 35 µL (2.0 mmol) of HF, 50 µL (0.6 mmol) of HNO_3 and 5 mL (277 mmol) of H_2O. The as synthesized MIL-100(Fe) was further purified by two-step processes using double solvent extraction with hot water and ethanol. In a typical purification process, 200 mg of hydrated solid was suspended into 100 mL of deionized water at 343 K for 3 hours and afterwards into 100 mL of ethanol at 338 K for 3 hours.

Adsorption and release of RAPTA-C from MIL-100(Fe)

Evacuation of MIL-100(Fe): Prior to the loading of RAPTA-C into MIL-100(Fe), the purified solid MIL-100(Fe) was heated at 473 K for 7 h and outgassed to 10^{-6} mbar. Under these conditions, the complete removal of the solvent guest molecules is achieved, obtaining empty pores ready for drug adsorption.

Loading of RAPTA-C at 298 K: The impregnation method was performed at 298 K by suspending 100 mg of activated MIL-100(Fe) into 10 mL of RAPTA-C solution prepared using absolute ethanol (0.086 M). The suspension was kept under stirring at room temperature and nitrogen atmosphere for 4 hours, in order to assure that equilibrium was reached. Afterwards, each sample was centrifuged in a Sigma 3-30K centrifuge (4000 rpm / 10min) using centrifuge tubes with a polyethersulfone (PES) membrane (Vivaspin 6, 30.000 kDa) in order to achieve the separation of MIL-100(Fe)@RAPTA-C loaded matrix from the solution by ultrafiltration. The MIL-100(Fe)@RAPTA-C loaded solid was washed three times with 10 mL of absolute ethanol to ensure that there was no free RAPTA-C on the external surface. The total amount of RAPTA-C incorporated into MIL-100(Fe) was indirectly calculated by monitoring the decrease of RAPTA-C concentration in the solution: UV-vis RAPTA-C absorption bands in absolute ethanol are found at 352 and 490 nm. The UV-vis data showed a maximum loading value of 0.95 mmol of RAPTA-C *per* mmol of MIL-100(Fe). When the impregnation process was repeated for 3 cycles, the consecutive impregnation did not lead to an improvement on the RAPTA-C adsorption capacity.

The total amount of RAPTA-C incorporated into the matrix was also calculated using Elemental and Thermogravimetric Analysis. *Anal. calc.* for $Fe_3O(H_2O)_2F(C_6H_3(CO_2)_3)_2(H_2O)_9(C_{16}H_{25}Cl_2N_3PRu)_{0.8}(C_6H_{12}PN_3)_{0.45}$ (MIL-100(Fe)@RAPTA-C): C, 32.05; H, 4.29; N, 4.18; *Anal. found*: C, 32.62; H, 6.28; N, 4.28.

Elemental analysis of MIL-100(Fe)@RAPTA-C indicates a significant loading capacity of RAPTA-C (Ru/Fe ratio = 0.27), close to 220 RAPTA-C molecules *per* unit cell (containing 816 Fe). As one unit cell contains 8 large and 16 small mesoporous cages,[3] one can estimate approximately 14 RAPTA-C molecules per large cage and 7 per small cage considering that RAPTA-C molecules occupy both cages with the same pore volume filling ratio.

Attenuated Total Reflectance (ATR) for RAPTA-C identification

The total amount of RAPTA-C incorporated into MIL-100(Fe) matrix was checked with Attenuated Total Reflectance (ATR). Different mixtures of MIL-100(Fe) (10 mg) and RAPTA-C (4, 8, 10 and 16 mg) were manually grinded and then deposited in the sample holder. It should be highlighted that the IR maximum absorption bands selected in this study are the ones where RAPTA-C has a maximum, while MIL-100(Fe) cannot adsorb (807, 973 and 1015 cm^{-1}). From the ATR results it can be concluded that there is 0.80 mmol of RAPTA-C per formula unit.

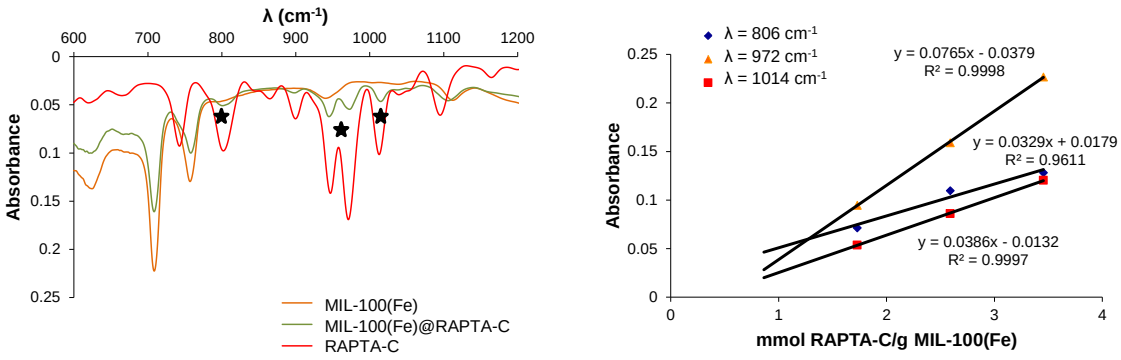

Figure S1. (Left) Representation of ATR data of the compounds MIL-100(Fe), MIL-100(Fe)@RAPTA-C and RAPTA-C. (Right) Linear fitting between sample absorbance and mmol of RAPTA-C *per* g of MIL-100(Fe)

IR spectrometry for RAPTA-C identification

RAPTA-C, MIL-100(Fe) and MIL-100(Fe)@RAPTA-C (2 mg) were manually grinded with dry potassium bromide in an agate mortar and then pressed into a disc. IR spectroscopic analysis clearly showed the presence of RAPTA-C into the MIL-100(Fe)@RAPTA-C loaded matrix.

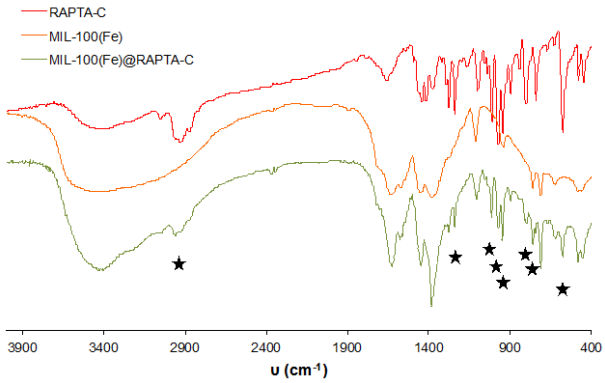

Figure S2. IR spectra of RAPTA-C, activated MIL-100(Fe) and MIL-100(Fe)@RAPTA-C samples

X-ray powder diffraction

XRPD measurements of the loaded MIL-100(Fe)@RAPTA-C confirmed that the crystal structure of the porous matrix is maintained.

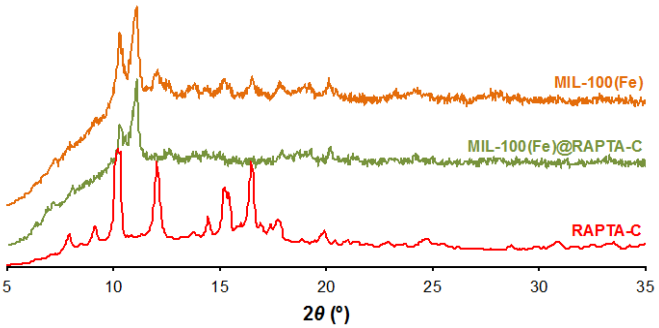

Fig. S3 XRPD patterns of activated MIL-100(Fe), loaded MIL-100(Fe)@RAPTA-C and RAPTA-C species

Thermal analysis

The thermal stability of free RAPTA-C, MIL-100(Fe) and MIL-100(Fe)@RAPTA-C samples was evaluated under an air stream.

Residue after thermal treatment of MIL-100(Fe)@RAPTA-C: $(Fe_3O_4)(RuO_2)_{0.8}$; *calculated*: 32.59%; *found*: 30.91%.

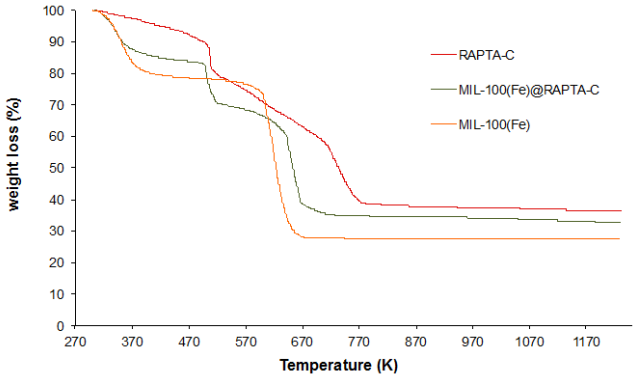

Figure S4. TG traces for RAPTA-C, MIL-100(Fe) and MIL-100(Fe)@RAPTA-C under air atmosphere

High Resolution Transmission Electron Microscopy

High Resolution Transmission Electron Microscopy (HR-TEM) and Energy-dispersive X-ray Spectroscopy (EDX) were performed using a STEM PHILIPS CM20 HR microscope equipped with an EDX spectrometer operating at an accelerating voltage of 200 keV. Samples were prepared by dispersing a small amount of the nanoparticles (3 mg) in absolute ethanol (1 mL), followed by sonication for 10 min and deposition on a copper grid. Nanoparticle size distribution was studied by HT-SEM using "ImageJ'' software for image processing and analysis.[4] The mean particle size was estimated from image analysis of *ca*. 200 particles at least. On the other hand, EDX analysis were performed in different locations in the sample and confirmed the presence of ruthenium and phosphorus in MIL-100(Fe)@RAPTA-C.

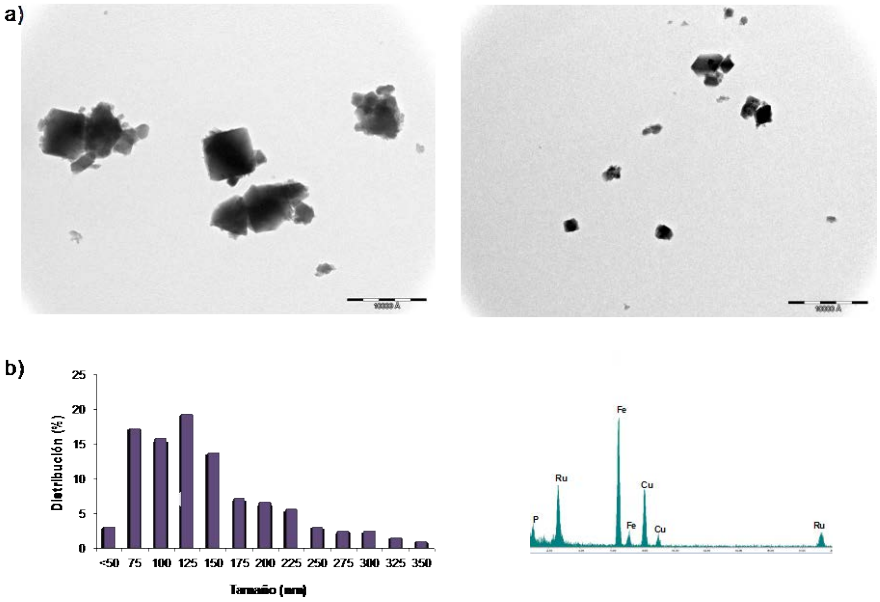

Figure S5. a) HR-TEM images of the sample MIL-100(Fe)@RAPTA-C. b) Results of the EDX quantitative analysis and particle size distribution.

Release of RAPTA-C

The delivery of RAPTA-C in Simulated Body Fluid (SBF) was studied at 310 K. SBF was prepared according to literature methods.[5] With this purpose, we prepared two solutions, A and B (Table S1) which were mixed just before each experiment in order to avoid the possible precipitation of some poorly soluble inorganic salts.

	Sol. A (g/L)	Sol. B (g/L)
NaCl	6.213	6.213
$NaHCO_3$	5.948	
KCl	0.450	
$Na_2HPO_4 \cdot 2H_2O$		0,498
$K_2HPO_4 \cdot 3H_2O$	0.462	
$MgCl_2 \cdot 6H_2O$	0.622	
$CaCl_2$		0.584
Na_2SO_4	0.144	

Table S1. Composition of the A and B solutions used for the preparation of the solution of simulated body fluid (SBF)

Quantification of RAPTA-C delivery and btc leaching by UV-vis

The study of RAPTA-C delivery and btc leaching process was carried out by suspending 10 mg of MIL-100(Fe)@RAPTA-C in 100 mL of SBF at 37 ^{o}C under stirring. Aliquots (3 mL) of the supernatant solution were analyzed by means of UV-vis at different periods of time (10, 20, 30, 45 min, 1, 1.5, 2, 2.5, 3, 4, 5, 7, 9, 11 hours, and 1, 1.16, 1.33, 1.45, 2, 2.16, 2.41, 3.25, 6 days) in order to determine the amount of released RAPTA-C, leached btc and the kinetics of the process. Each aliquot was centrifuged (4000 rpm / 1min) using centrifuge tubes with a polyethersulfone (PES) membrane (Vivaspin 6, 30.000 kDa), and then the solution and the solid were joined to the mother solution to keep the volume constant.

In SBF, UV-vis RAPTA-C absorption bands are found at 323 nm and 350 nm. These peaks are attributed to [Ru(*p*-cymene)Cl(H_2O)(pta)]$^+$ complex that is immediately obtained when RAPTA-C is hydrolyzed in water.[6] Moreover, the btc ligand leached during RAPTA-C delivery is soluble in SBF with its UV-vis maximum absorption bands at 214, 235 and 268 nm. Therefore, free btc ligand does not interfere with the UV-vis absorption of the RAPTA-C species which made possible to study the MIL-100(Fe) degradation.

Quantification of RAPTA-C delivery and btc leaching by RP-HPLC (measurement conditions)

Albumin (BSA) UV-vis absorption bands (204 and 273 nm) can interfere with the UV-vis absorption of the RAPTA-C species. RP-HPLC was used to study the release of RAPTA-C in both SBF media and SBF doped with BSA (5.4% w/v). Note that the albumin concentration was in the upper levels usually found in normal human physiological conditions (i.e. 3.5 – 5.0 % w/v) in order to better observe the impact of this serum protein over the RAPTA-C delivery.

The release of RAPTA-C and benzene-1,3,5-tricarboxilate (btc) was monitored, taking 0.2 mL aliquots of the supernatant solution, in a reversed phased HPLC system (RP-HPLC) using the same periods of time as in the case of the UV-vis studies. Standard solutions of RAPTA-C and btc were prepared in SBF or SBF supplemented with BSA for instrument response calibration. The chromatograms obtained by the HPLC method are shown in Figure S6. The identity of the RAPTA-C, btc and albumin was ascertained by their characteristic-UV-vis spectra with maximum

wavelengths at 203 and 301 nm; 212 nm; and 204 and 273 nm, respectively. The mobile phase used for the measurement consisted of a solution of methanol in a phosphate buffer (pH 3). The mobile phase was modified to optimise the separation between RAPTA-C, btc and albumin (BSA) resulting in a better determination of RAPTA-C, which consist in an isocratic mode 5:95 (v/v) (methanol – phosphate pH 3) (0 – 6 min) followed by a linear gradient to 5:95 (MeOH - water) (6-10 min). The flow rate was fixed to 0.8 mL min^{-1} and the injection volume was 20 µL. Finally, washing and reconditioning the column was done for 10 min. In all cases the column was operated at 37 °C and RAPTA-C, btc and BSA were monitored and quantified at 215 nm.

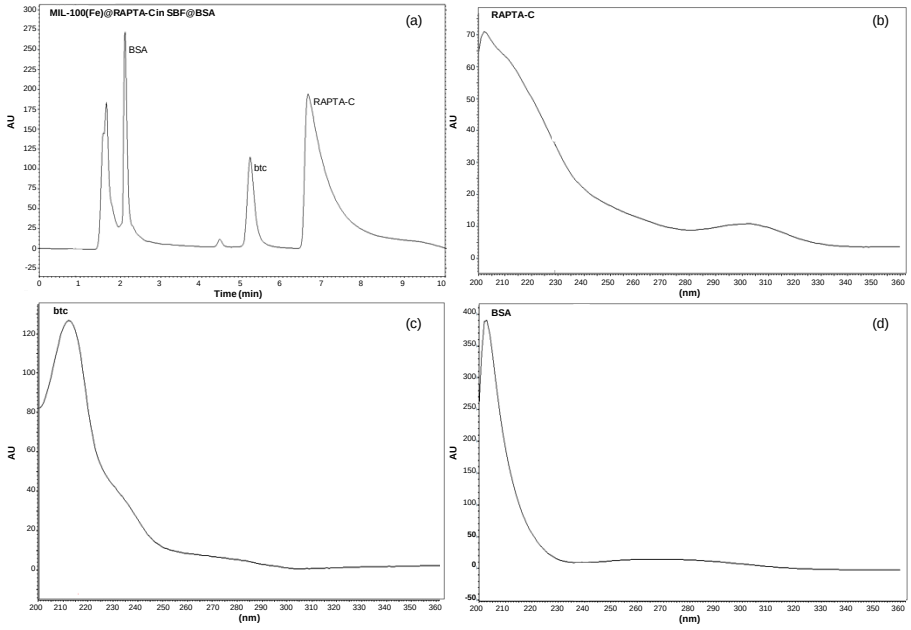

Figure S6. (a) Chromatograms of extract of MIL-100(Fe)@RAPTA-C in SBF doped with BSA. UV-vis spectrum of RAPTA-C (b), btc (c) and BSA (d) obtained by detection at 215 nm.

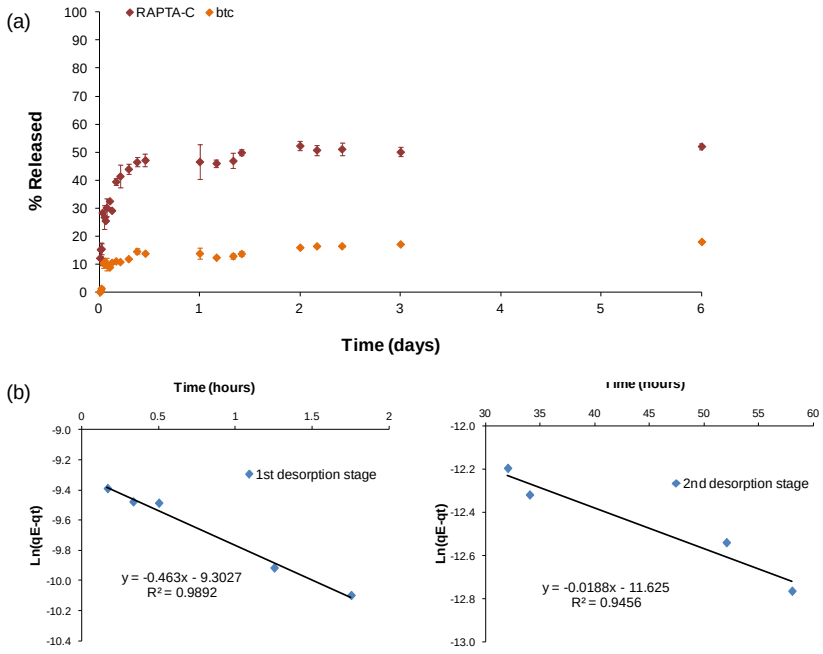

Figure S7. (a) Desorption kinetics profile of RAPTA-C (brown diamonds) and btc release (orange diamonds) from MIL-100(Fe)@RAPTA-C in SBF at 37 °C obtained by RP-HPLC. (b) Fitting of the data to a first order kinetic model for the 1st (left) and 2nd (right) desorption stage.

[1] C. S. Allardyce, P. J. Dyson, D. J. Ellis, S. L. Heath, *Chem. Commun.*, 2001, 1396-1397.

[2] Y. Seo, J. Yoon, J. Lee, U. Lee, Y. Hwang, C. Jun, P. Horcajada, C. Serre, J. Chang, *Microporous and Mesoporous Materials,* 2012, **157**, 137–145.

[3] R. Canioni, C. Roch-Marchal, F. Sécheresse, P. Horcajada, C. Serre, M. Hardi-Dan, G. Férey, J.-M. Grenèche, F. Lefebvre, J.-S. Chang, Y.-K. Hwang, O. Lebedev, S. Turner, G. Van Tendeloo, *J. Mat. Chem.*, 2011, **21**, 1226-1233.

[4] M.D. Abramoff, P.J. Magelhaes, S.J. Ram, *Biophotonics Int*., 2004, **11**, 36-42.

[5] T. Kokubo, H. Hushitani, C. Ohtsuki, S. Sakka, T. Yamamuro, *J. Mater. Sci.: Mater. Med*., 1992, **3**, 79-83.

[6] C. Scolaro, C.G. Hartinger, C.S. Allardyce, B.K. Keppler, P.J. Dyson, *J. Inorg. Chem.,* 2008, **102**, *1743-1748*.